International Journal of Aeronautical and Space Sciences
https://doi.org/10.1007/s42405-026-01196-6

IJASS International Journal of Aeronautical and Space Sciences

ORIGINAL PAPER

Hybrid Deep Learning Framework for Real-Time UAV Navigation with Adaptive Smoothness Control

P. Tamilselvi[1] · K. Jose Reena[2] · M. Vidhyasree[3] · V. Vishwa Priya[4]

Received: 18 August 2025 / Revised: 11 March 2026 / Accepted: 8 April 2026

Abstract
The objective of the study is to develop a reliable and energy-efficient urban UAV navigation system capable of overcoming GPS degradation, localization errors, dynamic obstacles, and inefficient flight trajectories by leveraging cellular network signals and advanced deep learning strategies. This research introduces a hybrid deep learning-based navigation system to enhance UAV reliability through cellular network signals. A multi-objective cost function is designed to optimize the uncertainty in motion, smoothness in trajectory, distance traveled, and the avoidance of collisions. A three-dimensional geometry-based channel propagation model (3DGCPM) is used to reduce the amount of inter-cellular interference. The federated meta multi-agent graph deep reinforcement learning (F2MGDRL) framework enables UAVs to adapt and learn in a decentralized and distributed manner by combining federated learning to allow for privacy-preserving decentralized training, meta-learning for fast adaptation to the changing environment in which the UAV is located. An adaptive enzyme action optimizer (AEAO) module provides for efficient and smooth trajectories with minimal abrupt turns. Experimental results show a success rate of 98.7% for completed missions and a latency of 45 s, and a significant improvement in the smooth and controlled movement of the UAV's trajectory. The system effectively navigates dynamic urban environments while minimizing energy consumption and abrupt maneuvers. The integration of cellular signals with a deep learning approach and adaptive control strategies mitigates the shortcomings of conventional GPS-based navigation systems and static navigation systems to deliver improved reliability, stability during flight, and improved operational efficiency.

Keywords UAV navigation · Adaptive smoothness control · Cellular network integration · Enzyme action optimizer · Multi-agent deep reinforcement learning

1 Introduction

Wireless ad hoc networks with UAVs are vital for applications such as environmental monitoring, surveillance, disaster management, and delivery due to their mobility and flexibility in harsh environments. Initially designed for military use, UAVs are now widely used in civilian sectors for their autonomy and maneuverability [1, 2]. Accurate UAV navigation is critical, but GPS-based systems face challenges in urban environments due to building blockages and signal degradation [3, 4]. Machine learning and deep reinforcement learning (DRL) approaches, like RRTs combined with CNNs, LSTMs, and attention mechanisms, show promise but struggle in complex dynamic settings [5]. Techniques like

Communicated by Fernando Tejero Embuena.

✉ P. Tamilselvi
tamizs2k2@gmail.com

K. Jose Reena
Joserheenaa@gmail.com

M. Vidhyasree
vidhyasreem56@gmail.com

V. Vishwa Priya
vishwapriya13@gmail.com

[1] Department of Computer Science and Engineering, Sathyabama Institute of Science and Technology, Chennai, Tamil Nadu 600119, India

[2] Department of Computer Applications, B. S. Abdur Rahman Crescent Institute of Science and Technology, Chennai, Tamil Nadu 600048, India

[3] Department of Artificial Intelligence, Panimalar Engineering College, Chennai, Tamil Nadu 600123, India

[4] Department Computer Science and Information Technology, Vels Institute of Science Technology and Advanced Studies, Chennai, Tamil Nadu 600117, India

Published online: 02 May 2026

DQNs and D3QN face limitations in adapting to continuous motion, especially under communication uncertainties and non-linear obstacles [6, 7].

Another significant problem in UAV navigation is to provide smooth, energy-efficient, and safe flight paths. High-curvature paths, sharp turns, and sudden changes in velocities and jerks cause energy consumption, flight instabilities, and collision risks. Although current DRL and optimization methods are beneficial for smoothness in flight paths, they are often limited in adapting to sudden changes in the environment in real time. Gaps are still present in optimizing smoothness, communication, collision avoidance, and efficient paths, especially in urban environments [8]. Centralized DRL approaches face scalability issues in multi-UAV systems, highlighting the need for decentralized learning. Many navigation strategies also fail to integrate communication models, like cellular signals. The proposed F2MGDRL+AEAO framework addresses these challenges by employing federated learning for decentralized updates, meta-learning for quick adaptability, and graph neural networks to model spatial interactions. Its multi-objective cost function optimizes motion uncertainty, smoothness, distance, and collision risk, while AEAO ensures stable, energy-efficient navigation with controlled jerk and curvature in complex environments.

2 Related Works

Optimal UAV navigation requires balancing coverage, connectivity, energy efficiency, and travel time. However, existing methods, including heuristic, mathematical, machine learning (ML), and metaheuristic approaches, have limitations in providing robust, scalable, and efficient solutions. Afifi and Gadallah [9] proposed a double deep Q-network (DDQN)-based framework for real-time UAV guidance, addressing kinematic and dynamic models. However, challenges remain in integrating multi-modal learning for cooperative UAV navigation and optimizing long mission energy usage. Tonti et al. [10] utilized proximal policy optimization with long short-term memory (PPO+LSTM) for energy optimization and noise reduction in 2D fluid flow simulations. However, 3D dynamics and obstacles at varying heights posed challenges. Zhang et al. [11] introduced a reinforcement learning-based cooperative navigation (RL-CN) algorithm with dual sub-actor networks for improved decision-making in dense scenarios, though decentralized control for large UAV swarms remained problematic. Ren et al. [12] developed the K-means online learning routing protocol (K-MORP) using a 3D Gauss–Markov mobility model to optimize routing, load balancing, and clustering in UAV ad hoc networks, but advanced learning techniques were needed for better energy and routing optimization.

Meng et al. [13] proposed a robust indoor UAV localization system using factor graph optimization (FGO) combined with a two-phase CNN for classification and noise estimation. However, UWB signal degradation indoors led to significant range and positioning errors. Tricomi et al. [14] introduced the integrated multilateral mobility framework for smart cities, using the CV POp-CoRN system, but faced challenges in gaining citizens' trust and effectively implementing smart contracts. Pasandideh et al. [15] optimized UAV base station (UAV-BS) placement using mixed-integer nonlinear programming (MINLP), though the optimal number of UAV-BSs for cost-effective deployment remains unresolved. Tutsoy et al. [16] proposed minimum distance and minimum time 3D path planning algorithms using modified particle swarm optimization (PSO) and genetic algorithms (GA), but lacked multi-UAV coordination and were sensitive to battery constraints. The proposed F2MGDRL framework addresses these limitations by offering adaptive real-time UAV navigation, and AEAO refines trajectories for dynamic smoothness control. This integration ensures energy-efficient, collision-free, communication-effective, and smooth UAV operations, even in complex and dynamic environments, overcoming the challenges seen in prior solutions.

2.1 Research Gap

The GPS-based UAV navigation is affected in an urban area due to signal degradation, blockage, and multipath effects, resulting in position errors and mission failure. The UAV trajectory is obtained with abrupt and inefficient paths. The learning models are not effective in adapting to changing scenarios. The real-world UAV operations are affected by various uncertainties such as time-varying dynamics, non-linearities, wind effects, and communication channel variations. The proposed F2MGDRL framework is effective in overcoming the challenges faced by the UAV navigation systems. The proposed framework is based on meta-learning, GNN-based spatial modeling, and smoothness control using AEAO. The channel modeling and multi-objective optimization are effectively integrated into the proposed framework.

2.2 Contributions

- The F2MGDRL framework is developed by integrating federated learning, meta-learning, and graph neural networks. This enables decentralized, private, and ultra-adaptable navigation of UAVs in urban environments. The framework efficiently handles the complex spatial interactions of UAVs, obstacles, and communication links.
- The multi-objective cost function of trajectories is built to optimize various parameters like motion uncertainty, smoothness of trajectories, distance of trajectories, and collision avoidance. The integration of 3DGCPM into

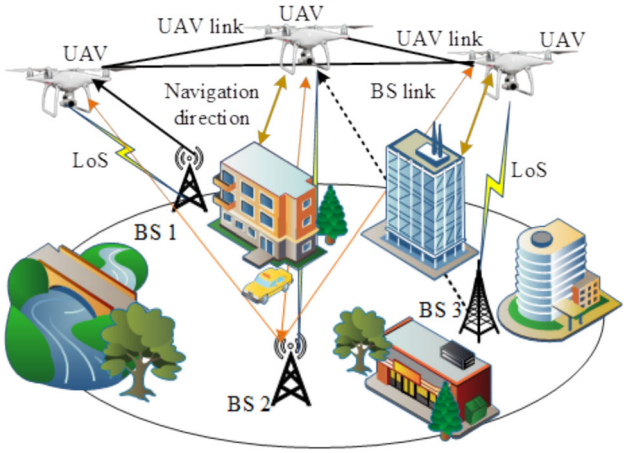

Fig. 1 UAV navigation over cellular network

this framework enables effective reduction of intercell interference as well as communication-aware navigation reliability.

- An AEAO-based smoothness control module has been developed to enhance the smoothness of the trajectory bounds, achieve rapid convergence, and address non-linear constraints. This module controls the jerk, curvature, and acceleration of the UAV motion, ensuring smooth and efficient motion in complex and cluttered urban environments.

The organization of this research is as follows: Sect. 2 presents the related work, while Sect. 3 presents a detailed description of the methodology. Section 4 presents the experimental analysis of the research, followed by a discussion in Sect. 5. The conclusion of the research and future work are presented in Sect. 6.

3 Proposed Methodology

This research presents a hybrid deep learning-based framework for real-time UAV navigation, integrating F2MGDRL for adaptive trajectory planning, 3DGCPM for intercell interference mitigation, and AEAO for adaptive smoothness control. The framework operates in three stages: first, 3DGCPM models the communication environment by estimating the Line-of-Sight (LoS) probability and communication reliability.

Next, F2MGDRL employs federated reinforcement learning for decentralized trajectory planning. Finally, AEAO refines the generated trajectories by minimizing jerk, curvature, and acceleration variations. Figure 1 illustrates the communication between UAVs and base stations (BS1, BS2, BS3), with each UAV following its planned path for smooth, stable, and collision-free navigation in urban environments.

To formally define the navigation task, the UAV state is represented as $s_t = [x_t, y_t, z_t, v_t, a_t, \theta_t, \varphi_t]$, where x_t, y_t, z_t are the UAV position coordinates, v_t is the velocity, a_t is the acceleration, and θ_t, φ_t are the pitch and yaw angles of the UAV and the control action as $u_t = [\Delta v_t, \Delta\theta_t, \Delta\varphi_t]$, representing the change in velocity and orientation at time t. The trajectory planning minimizes the unified cost function that considers smoothness, distance, uncertainty, and collision risk, subject to acceleration, jerk, and 3DGCPM-based communication constraints. The optimal policy π guarantees real-time dynamics and feasibility that are closely consistent with the framework's mathematical formulation.

3.1 3D Geometry-Based Channel Propagation Model for UAV Communication

The 3DGCPM [17] reduces intercell interference by modeling PLoS with parameters like UAV altitude, elevation, and azimuth angles, as well as urban structural parameters. First, it finds the maximum blocking height of a building given the elevation angle (θ), as well as street width, as shown in Eq. (1):

$$H_{b\max 1} = W \times \tan(\theta) \tag{1}$$

where $H_{b\max 1}$ represents a maximum building height blocking LoS, W is the street width, and θ is the elevation angle between the UAV and UE. This estimation identifies critical urban structural limits affecting UAV communication reliability. To determine the probability of LoS for a single building, the model uses a closed-form expression that incorporates the statistical distribution of building heights in the environment, as denoted in Eq. (2):

$$P^{s}_{LoS}(\theta, W, B) = 1 - \sqrt{\frac{\pi}{2}}\frac{\gamma}{H_{b\max 1}} erf\left(\frac{H_{b\max 1}}{\sqrt{2\gamma}}\right) \tag{2}$$

where $P^{s}_{LoS}(\theta, W, B)$ is the probability of LoS for a single building, B indicates a building width γ is the scale parameter of the Rayleigh distribution representing building height variability, and erf is the error function. In dense urban environments, multiple buildings obstruct the UAV-to-UE path, requiring a generalized formulation to estimate LoS probability along the entire propagation path. Then, the model considers the azimuth angle φ UAV and UE, which scales the effective street width and building width in order to obtain the azimuth aware LoS probability in Eq. (3).

$$P^{ri}_{LoS}(\theta, W, B, \varphi) = \prod_{i=1}^{n} P^{S}_{LoS}(\theta, X_{ri}\prime, w\prime)_i \tag{3}$$

where ri denotes a region, φ is the azimuth angle, and $X_{ri}\prime$, $w\prime$ are the effective street and building widths considering azimuth alignment. Finally, the overall 3D PLoS across all urban regions is calculated to provide a comprehensive measure of LoS availability in the UAV communication environment, as represented in Eq. (4):

$$P_{LoS}(\theta,\ W,\ B) = \frac{WB}{A}\left(P_{LoS}^{r1} + P_{LoS}^{r2}\right) + \frac{W^2}{A}\left(P_{LoS}^{r3}\right) \quad (4)$$

where P_{LoS}^{r1}, P_{LoS}^{r2} and P_{LoS}^{r3} represent LoS probabilities in different urban regions. This 3DGCPM framework is used for the optimization of UAV trajectory planning and communication optimization under realistic urban propagation conditions, thus reducing intercell interference while considering the dynamic and kinematic constraints of the UAV.

3.2 Reinforcement Learning Integration

The F2MGDRL model enables UAV navigation in dynamic environments by generating real-time, smooth, and collision-free trajectories. It integrates FL for decentralized training, meta-learning for fast adaptation, and graph neural networks (GNN) to capture spatial relationships between UAVs and obstacles. The training occurs in two stages: an offline phase where UAVs collect data and update local policy networks, followed by federated averaging to form a global model, and an online phase where real-time inference is performed using local observations processed through the GNN.

3.2.1 Federated Learning Model Training

FL [18] enables decentralized learning by allowing each UAV to train locally on its own navigation (N) data while sharing only model parameters with a central aggregator. The parameters from federated averaging in Eq. (5) combine to create a global model which maintains data privacy while enhancing security and enabling efficient collaborative learning among UAVs without transmitting raw flight data:

$$N(u_1,\ u_2,\ \ldots,\ u_V) = \frac{1}{V}\sum_{i=1}^{V}\lambda_i(u_i) \quad (5)$$

where u_i represents the weights of the local model trained by UAV λ_i on the device i, and V denotes the total number of participating UAVs. The collaborative learning strategy allows UAVs to share model updates while preserving data privacy, minimizing communication overhead, and ensuring efficient learning, real-time responsiveness, and stable fleet coordination every 100 rounds.

3.2.2 Meta-learning for Rapid Adaptation

Meta-learning enables rapid UAV adaptation by learning a transferable initialization that quickly adjusts to new environments. Using MAML [19], task-specific gradients update parameters as in Eq. (6), ensuring fast trajectory prediction and efficient real-time navigation across diverse conditions:

$$\hat{\theta} = \text{Ø-}\ \alpha\nabla_{\text{Ø}}L\left(\text{Ø}\right) \quad (6)$$

where $\hat{\theta}$ is an updated parameter, Ø is a meta-initialized parameter, α is a learning rate for a task-specific update, and $L\left(\text{Ø}\right)$ represents a loss for a task under the model. This process enables strong generalization from limited data by optimizing a meta-objective that minimizes the summed post-update losses across sampled tasks. The meta-gradient in Eq. (7) refines the initialization, ensuring rapid adaptation and high performance on new tasks β:

$$\text{Ø} \leftarrow \text{Ø-}\ \beta\nabla_{\text{Ø}}L\left(\text{Ø}\right) \quad (7)$$

where β is a meta-learning rate dictating the update of an outer loop. The meta-learning module allows rapid UAV adaptation by fine-tuning 20 MB of shared parameters within 8–10 s for real-time responsiveness. GNNs [20] model UAVs and obstacles as nodes, capturing local avoidance and global swarm coordination, supporting robust, collision-free, and efficient trajectory planning. The framework of F2MGDRL is represented in Fig. 2.

The GNN module enables UAVs to exchange local observations every 50 ms, allowing each node to aggregate features from nearby UAVs and obstacles for spatially informed decision-making. This ensures real-time situational awareness, coordinated trajectory planning, and avoidance of conflicts. The communication frequency is optimized to balance rapid environmental updates with low communication overhead, supporting stable and efficient multi-UAV navigation.

3.2.3 Multi-agent Deep Reinforcement Learning for Real-Time Navigation

The system employs multi-agent deep reinforcement learning (MADRL) [21] with a decentralized partially observable Markov decision process (Dec-POMDP) framework for controlling multiple UAVs in dynamic environments. Using local data like directional angles and rangefinder readings, the MARDPG system incorporates LSTM networks for enhanced policy development. The UAV is modeled as a quadrotor with basic kinematic movements, with state

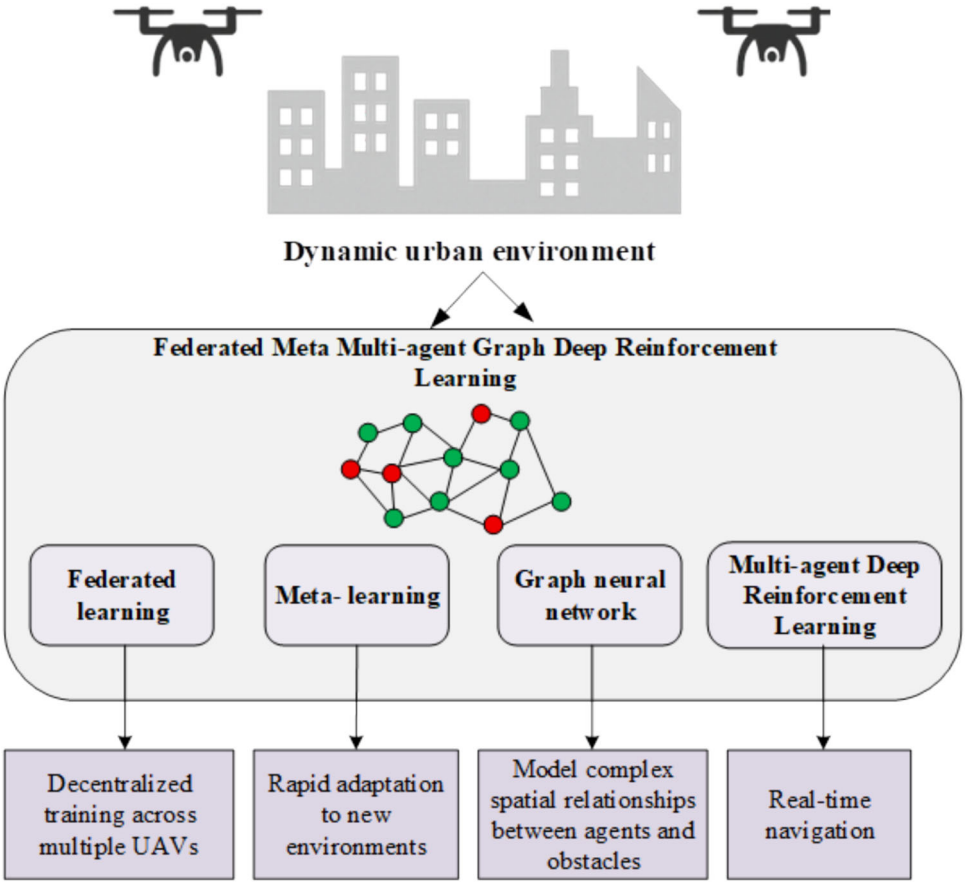

Fig. 2 Framework of F2MGDRL

updates in Eq. (8):

$$\begin{cases} h_{t+1} = h_t + \rho_t \\ v_{t+1} = v_t + \tau_t \\ p_{t+1} = p_t + h_t \times \cos(h_{t+1})\cos(v_{t+1}) \\ q_{t+1} = q_t + h_t \times \sin(h_{t+1})\cos(v_{t+1}) \\ s_{t+1} = s_t + h_t \times \sin(v_{t+1}) \end{cases} \tag{8}$$

where h_t and v_t denote the horizontal and vertical angles of UAV at time t, ρ_t and τ_t represent a steering signal for angles at time t, and p_t, q_t and s_t describe a UAV's position coordinates at time t. Each UAV's observation space includes directional angles, rangefinder perceptions, and the relative position to the target point. Although the implementation applies standard MADRL, the MARDPG algorithm serves as an advanced variant, incorporating LSTM networks to utilize historical trajectories. Its policy gradient update for agent is expressed in Eq. (9):

$$\nabla_{\theta_i} B(\mu_i) = \mathrm{E}_{u(G)}\Big[\nabla_{\theta_i}\mu_{\theta_i}\big(x_{i,t}\big|g_{i,t}\big)\nabla_{x_i,t}G_i^{\mu} \big(g_{1,t},\ \ldots,\ g_{N,t},\ x_{1,t},\ \ldots x_{N,t}\big|x = \mu_{\theta_i}\big(g_{1,t,\ldots,g_{N,t}}\big)\big)\Big] \tag{9}$$

where θ_i is a parameter of agent i policy network, $\mathrm{E}_{u(G)}$ is an expectation over minibatch samples drawn uniformly from replay buffer, $B(\mu_i)$ illustrates an expected return objective for agent i, μ_{θ_i} represents a policy function of agent i, $x_{i,t}$ signifies an action done by agent i at time t, $g_{i,t}$ is an observation history of agent, G_i^{μ} denotes a critic function for agent i, $g_{1,t}$, ..., $g_{N,t}$ indicates an observation history of all agents, and $x_{1,t}$, $\ldots x_{N,t}$ describes the actions of all agents. The reward function is designed to ensure collision avoidance, target approach, smooth navigation, and energy efficiency, as mentioned in Eq. (10):

$$R_t = w_1 R_{target} + w_2 R_{collision} + w_3 R_{smooth} + w_4 R_{explore} \tag{10}$$

where R_{target} denotes rewards approaching the target, $R_{collision}$ penalizes proximity to obstacles, R_{smooth} encourages smooth motion and trajectory stability, $R_{explore}$ rewards safe exploration of the environment, and w_1,w_2,w_3,w_4 are weighting coefficients controlling the importance of each term. The reward function provides a dense feedback signal for the agent, accelerating convergence and guiding safe, efficient trajectory planning in dynamic urban environments. The actor-critic parameter updates for an agent i are given in

Eq. (11):

$$\theta_i \leftarrow \theta_i + \alpha \cdot \nabla_{\theta_i} J(\theta_i) \tag{11}$$

where θ_i represents a parameter of an agent's $(i)\left(\frac{i}{a}\right)$ policy network, αQ^c is a learning rate, and $\nabla_{\theta_i} J(\theta_i) \nabla_{\theta_i} J(\theta_i)$ is a gradient of an objective function $J(\theta_i) J(\theta_i)$ with respect to a policy parameter. The actor optimizes UAV policy actions for maximum return, while the critic minimizes temporal-difference errors, ensuring stable learning. Together, they enable adaptive, collision-free, and smooth navigation in dynamic urban environments. The critic network loss function $(L(\theta_i))$ $((mathcal I(\theta_i)))$ is defined in Eq. (12):

$$L(\theta_i) = \mathrm{E}_{u(G)}\left[\left(G_i^{\mu}\left(g_{1,t}, \ldots g_{N,t}, x_{1,t}, \ldots, x_{N,t}\right) - y_{i,t}\right)^2\right] \tag{12}$$

where G_i^{μ} is a current critic value estimate, and $y_{i,t}$ denotes a target critic value. The multi-objective cost function minimizes travel distance, smoothness deviation, collision risk, motion uncertainty, and communication loss, with 3DGCPM adding a communication penalty. AEAO refines smoothness, enabling real-time, scalable, and stable UAV navigation in highly dynamic urban environments.

3.3 Adaptive Smoothness Control

The F2MGDRL framework incorporates an adaptive control module to regulate UAV trajectory smoothness using real-time feedback. The AEAO [22] refines the policy outputs from F2MGDRL, adjusting trajectory points to minimize jerk, curvature, and acceleration variations. A multi-objective fitness function evaluates candidate trajectories, selecting the optimal path that ensures smooth, stable, and energy-efficient navigation, with an initialization population detailed in Eq. (13):

$$A_i^{(0)} = lb + (ub - lb)\Theta v_i \tag{13}$$

where $A_i^{(0)}$ represents an initial position of i^{th} search agents, lb and ub indicates a lower and upper bound, and v_i denotes a random vector. The adaptive factor (Af_t) for iteration t is calculated in Eq. (14):

$$Af_t = \sqrt{\frac{t}{Max\,iter}} \tag{14}$$

The adaptive factor progressively increases while remaining controlled, allowing the adaptation rate to respond to system states and enhance path smoothness. The fitness function from Eq. (15) evaluates each candidate trajectory by measuring three elements, which are smoothness and distance, and collision avoidance, and these three elements support the global optimization goal that the critic loss in Eq. (12) establishes:

$$F(A) = Minimize(loss(w1 \times D(X) + w2 \times C(X) + w3 \times S(X))) \tag{15}$$

where $D(X)$ represents the travel distance, $C(X)$ describes the collision avoidance cost, $S(X)$ indicates the smoothness cost, and $w1$,$w2$,$w3$ are the weights. The fitness function integrates travel distance, collision avoidance, and smoothness $S(X)$, guiding UAVs to select the shortest, safest, and smoothest paths. Incorporating UAV motion constraints in AEAO ensures minimized abrupt turns, enhancing energy efficiency, flight stability, and overall navigation performance. These constraints include a maximum jerk limit $j(t) \le j_{\max}$, maximum acceleration limit $a(t) \le a_{\max}$, and a curvature bound defined in Eq. (16):

$$k(t) = \frac{x'(t)y''(t) - y'(t)x''(t)}{\left(x'(t)^2 + y'(t)^2\right)^{3/2}}, \quad k(t) \le k_{\max} \tag{16}$$

where $x'(t)$,$y'(t)$ are the UAV's velocity components, $y''(t)$,$x''(t)$ are the UAV's acceleration components, $k(t)$ measures how sharply the path bends, and $k_{\max}$ is the maximum allowable curvature. A higher curvature value is associated with a sharp or abrupt turn. At each iteration t, the objective function values of both candidate positions are evaluated. The better position between these two candidates is selected as the updated candidate position, as defined in Eq. (17):

$$A_{i,update}^{(t)} = \begin{cases} A_{i,1}^{(t)}, & if\ F\left(A_{i,1}^{(t)} < F\left(A_{i,2}^{(t)}\right)\right) \\ A_{i,2}^{(t)}, & otherwise \end{cases} \tag{17}$$

where $A_{i,update}^{(t)}$ represents an improved candidate position and $F(.)$ indicates an objective function. In AEAO, substrate positions are constrained within bounds to ensure feasible solutions. Iterative minimization of curvature and jerk refines F2MGDRL paths, producing smooth, energy-efficient, and collision-free UAV trajectories suitable for complex urban environments. The framework defines clear state representations, reward functions, optimization constraints, and communication parameters, with the RL policy network controlling velocity and direction while AEAO enforces jerk, acceleration, and curvature limits.

Table 1 Experimental parameter settings

Parameters	Values
UAV maximum jerk	10 m/s^3
UAV maximum acceleration	5 m/s^2
Data size per UAV	2000
Central frequency	5 GHz
No. of source: destination UAVs	10–100 UAVs
Rounds of FL training	100
UAV average speed	15 m/s
Propagation model	3DGCPM
Optimizer	Adaptive enzyme action optimizer
Cellular communication range	1500 m
Communication frequency	Updates every 100 rounds
Model size per UAV	20 MB
Computational requirements per UAV	10 s per training round
Static obstacles	10, 20, 30, 40 (mapped to complexity levels 1–4)
Dynamic obstacles	5, 10, 15, 20 (mapped to complexity levels 1–4)
Obstacle shapes	Cuboid (5–20 m), cylindrical (radius 2–8 m)
UAV initial distribution	Uniform random across 2 km × 2 km grid
UAV goal distribution	Opposite-quadrant destination assignment
Environment complexity levels	Level 1 (low obstacles, low NLOS), Level 2 (moderate obstacles, moderate NLOS), Level 3 (high obstacles, high NLOS)
NLOS conditions	Low, moderate, high
Wind speed	0–10 m/s
Obstacle location type	Random/fix locations
Transmission power	10 dBm

4 Experimental Outcome Analysis

The experimental analysis evaluates key metrics such as trajectory smoothness, collision avoidance, and communication reliability based on the proposed cost function. The F2MGDRL framework demonstrates improved optimization performance in real-time conditions. Simulations were implemented in Python 3.11 using Anaconda and Spyder on an Intel Core i7-6700 CPU with 16 GB RAM. The experiments were conducted in a 2 km × 2 km grid environment with UAV swarm sizes ranging from 10 to 100 agents, navigating between assigned points under varying obstacle densities and environmental conditions. Training involved 100 federated learning rounds with periodic model synchronization. Table 1 outlines the parameter settings.

The results show that the proposed framework outperforms existing methods consistently, with federated learning and deep reinforcement learning running offline on edge servers, while UAVs perform online inference. The system achieves an average decision-making time of 15–20 s, ensuring alignment with standard control-loop limits and UAV platform capabilities.

4.1 Performance Evaluation

The assessment tested the system across multiple trials and ablation studies, demonstrating consistent performance and resilience against dynamic obstacles, NLOS conditions, and multi-UAV interference, ensuring reliable real-world operation.

Navigation results analysis

The navigation results analysis evaluates the performance of the proposed approach by comparing trajectory accuracy, reliability, and overall effectiveness with existing methods in dynamic environments.

Figure 3a demonstrates the superiority of F2MGDRL-AEAO, achieving the lowest MSE from 0.10 at 20 UAVs to only 0.25 at 90 UAVs, while competing methods rise sharply to 1.10–1.55. The results in Fig. 3b show that the system produces its shortest trajectory lengths, which are 97 m, 74 m, and 70 m, thus proving that it creates smoother and more efficient paths.

Table 2 shows the performance of various methods across different environmental complexity levels. Level 1 has fewer static and dynamic obstacles with lower NLOS interference,

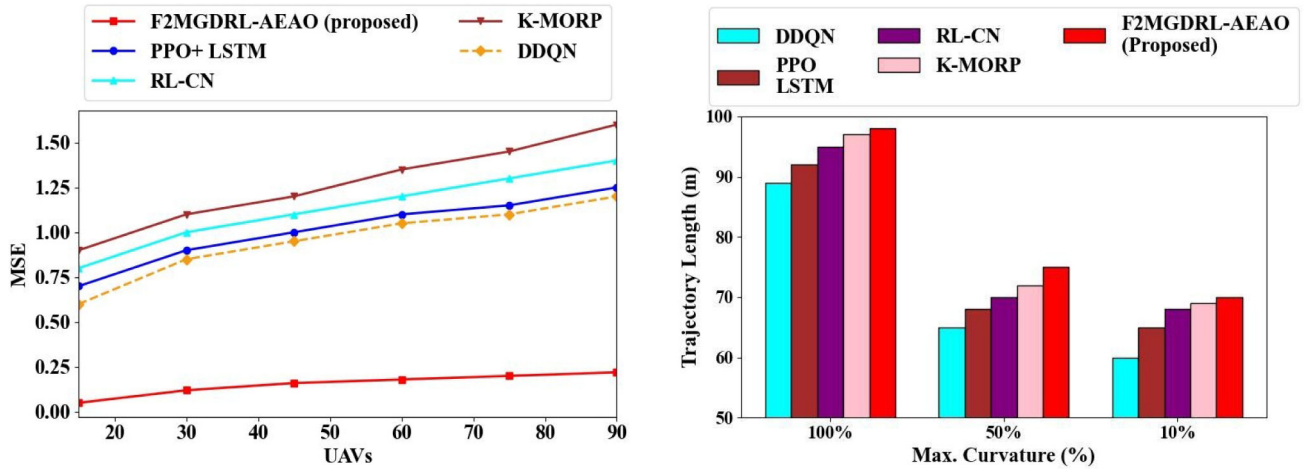

(a) (b)

Fig. 3 Performance comparison: **a** MSE, **b** trajectory length

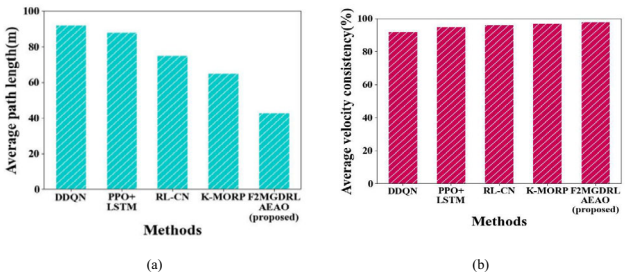

(a) (b)

Fig. 4 Navigation performance comparison: **a** average path length, **b** average velocity consistency

while Levels 2–4 progressively increase the complexity. As the environment becomes more challenging, the F2MGDRL-AEAO method consistently outperforms others in mission success rate, collision rate, and path length. In contrast, the other methods experience significant performance degradation as the complexity level increases.

Figure 4 depicts the navigation performance comparison. In Fig. 4a, for average path length, DDQN [9] reports 95 m, PPO+LSTM [10] reports 85 m, RL-CN [11] reports 70 m, and K-MORP [12] reports 60 m, whereas F2MGDRL-AEAO reports the shortest path length at 40 m. For average velocity consistency (%), in Fig 4b, DDQN reports 90%, PPO+LSTM reports 92%, RL-CN reports 95%, and K-MORP reports 97%, whereas F2MGDRL-AEAO reports the highest velocity at 99%, demonstrating superior velocity stability during navigation.

Adaptive smoothness analysis

This section presents the evaluation and performance analysis of the proposed adaptive smoothness control approach. This approach is quite effective in generating stable, smooth, and feasible UAV trajectories.

Table 3 presents a comparison of UAV trajectory smoothness and adaptive control metrics across different optimization algorithms. The crested porcupine optimizer (CPO), artificial protozoa optimizer (APO), pied kingfisher optimizer (PKO), and the proposed AEAO are evaluated. The AEAO achieves the lowest mean jerk and path deviation, along with the shortest trajectory length, demonstrating smoother, more stable paths and higher reliability, highlighting its superior performance for UAV navigation tasks.

Table 4 compares centralized MADDQN, centralized MADRL, and the proposed F2MGDRL-AEAO. The F2MGDRL-AEAO outperforms both baselines with a 98.7% mission success rate, lower collisions, smoother and shorter trajectories, and faster convergence, achieving 90% success in 110 episodes versus 180–220 for centralized methods, demonstrating the advantages of federated meta-learning and GNN cooperation for real-time UAV trajectory planning.

Table 5 displays that the increasing environment complexity significantly lowers the performance of the centralized methods; at Level 4, Centralized-MADDQN drops to 80.3%, while F2MGDRL-AEAO maintains a 93.4% success rate with lower collision levels, which testifies to stronger robustness, scalability, and adaptability compared to centralized approaches.

Table 6 summarizes the averaged results over multiple independent runs with fixed random seeds to ensure statistical reliability across all communication channel conditions. The proposed F2MGDRL-AEAO yields higher success rates, lower MSE, and smoother trajectories with smaller variances compared to DDQN [9] and RL-CN [11], thus manifesting stability, generalizing better to dynamic 3D environments, and turning out more reliable in decision-making under uncertainty.

Table 2 Performance with environment complexity levels

Environment complexity level	Concrete environment definition	Avg. success rate (%)			Avg. collision rate (%)			Avg. path length (m)		
		RL-CN [11]	DDQN [9]	F2MGDRL-AEAO (proposed)	RL-CN [11]	DDQN [9]	F2MGDRL-AEAO (proposed)	RL-CN [11]	DDQN [9]	F2MGDRL-AEAO (proposed)
Level 1	10 static + 5 dynamic obstacles; 10 UAV pairs; low NLOS	95.0	91.0	98.0	54	57	30	79	76	70
Level 2	20 static + 10 dynamic obstacles; 25 UAV pairs; moderate NLOS	93.0	89.0	97.0	64	65	40	85	86	76
Level 3	30 static + 15 dynamic obstacles; 50 UAV pairs; high NLOS	90.0	85.0	95.0	74	75	50	88	90	85
Level 4	40 static + 20 dynamic obstacles; 100 UAV pairs; very high NLOS	86	80	93	84	79	70	92	97	87

Table 3 UAV smoothness metrics analysis

Algorithms	Mean jerk (m/s^3)	Jerk Std Dev (m/s^3)	Mean path deviation (m)	Path deviation Std Dev (m)	Mean smoothness index	Smoothness Std Dev	Trajectory length (m)	Max curvature (%)	Computation time (s)
CPO [23]	1.42	0.06	0.68	0.04	0.72	0.02	85.3	0.72	102.4
APO [24]	1.36	0.05	0.64	0.03	0.75	0.02	87.5	0.75	35.6
PKO [25]	1.29	0.04	0.61	0.03	0.77	0.01	86.2	0.70	29.4
AEAO (proposed)	1.12	0.03	0.53	0.02	0.83	0.01	83.9	0.66	24.2

Table 4 Fair performance comparison under identical training budget and conditions

Metric	Centralized-MADDQN	Centralized-MADRL	F2MGDRL-AEAO (proposed)
Mission success rate (%)	87.3	89.4	98.7
Collision rate (%)	18.6	14.8	4.6
Avg. path length (m)	61.5	58.2	43.1
Average trajectory error (m)	1.62	1.41	0.92
Smoothness index	0.68	0.71	0.86
Processing time (s)	54.3	51.2	45
Real-time responsiveness (ms)	50.7	49.3	43.1
Convergence episodes (90% success)	220	180	110

Table 7 presents a comparison of the performances of DDQN [11], RL-CN [13], and F2MGDRL-AEAO under realistic cellular network environments. It is observed that the communication delays for F2MGDRL-AEAO are the lowest, along with minimal packet loss and handover cases. This indicates the robustness of the F2MGDRL-AEAO approach for providing stable UAV navigation through the cellular network.

Table 8 demonstrates the scalability of the F2MGDRL-AEAO framework across varying UAV swarm sizes. The method maintains high mission success rates (above 97.2%) even with 100 UAVs, ensuring reliable coordination and collision avoidance. Path lengths increase marginally (41.7–46.0 m), while trajectory error remains low (0.83–1.00 m) and the smoothness index stays above 0.84. Although the collision rate rises slightly (3.6–5.2%), these results highlight the framework's efficient, scalable, and safe multi-UAV navigation.

Table 9 presents a computational complexity analysis of the proposed F2MGDRL-AEAO method compared to existing approaches. The F2MGDRL-AEAO method achieves a computation time of 24.5 s, which is lower than DDQN (35.4 s) and PPO+LSTM (38.2 s). It utilizes 38.5 GFLOPs and 2.9 million parameters, while optimizing energy consumption at 10.2 J and requiring 45 MB of memory. These trade-offs enhance scalability and adaptability, making the method well suited for decentralized UAV navigation in dynamic environments.

4.2 Ablation Study

In the present research, an ablation study is conducted to evaluate the contribution of each of the major components in the proposed F2MGDRL framework by deleting or replacing each of the major modules in turn.

As shown in Table 10, each component in the proposed F2MGDRL framework, namely FL meta-learning, GNN, and AEAO, improves performance significantly. Removing any module increases trajectory error, reduces smoothness, and lowers mission success. The complete F2MGDRL achieves a 98.7% mission success rate, and 0.92 m trajectory error, reflecting improved computational efficiency and real-time responsiveness.

Table 5 Environment complexity comparison between centralized and federated approaches

Env level	Method	Success rate (%)	Collision rate (%)	Avg. path length (m)	MSE	Smoothness index
Level 1	MADDQN	92.4	11.3	56.8	0.87	0.69
	MADRL	94.1	9.2	52.4	0.74	0.73
	F2MGDRL-AEAO	98.5	3.1	38.7	0.52	0.85
Level 2	MADDQN	89.5	14.7	63.3	1.02	0.67
	MADRL	90.3	12.5	60.8	0.89	0.70
	F2MGDRL-AEAO	97.3	5.4	44.5	0.61	0.83
Level 3	MADDQN	85.7	17.6	71.9	1.30	0.65
	MADRL	87.8	15.8	68.4	1.12	0.69
	F2MGDRL-AEAO	95.2	7.1	50.1	0.78	0.81
Level 4	MADDQN	80.3	20.1	79.2	1.62	0.61
	MADRL	82.5	18.3	76.1	1.45	0.67
	F2MGDRL-AEAO	93.4	9.5	58.7	1.02	0.79

Table 6 Statistical results across multiple runs

Method	Success rate (mean ± SD)	MSE (mean ± SD)	Trajectory smoothness (mean ± SD)
DDQN [9]	0.82 ± 0.04	0.137 ± 0.012	0.214 ± 0.018
RL-CN [11]	0.87 ± 0.03	0.119 ± 0.009	0.196 ± 0.015
F2MGDRL-AEAO (proposed)	0.94 ± 0.02	0.091 ± 0.007	0.142 ± 0.010

Table 7 Communication performance comparison under cellular network conditions

Method	Avg. communication delay (ms)	Packet loss rate (%)	Handover events per mission
DDQN [9]	120	3.5	8
RL-CN [11]	105	2.8	6
F2MGDRL-AEAO (proposed)	95	1.5	4

5 Discussion

The proposed F2MGDRL-AEAO framework consistently outperforms in navigation accuracy, communication efficiency, smoothness, and robustness across various UAV densities and environmental complexities. Figure 3 shows high throughput and low delay, while Fig. 4 confirms minimal MSE and reduced trajectory length. Table 2 shows strong generalization with higher success rates and lower collision levels under NLOS conditions. The adaptive smoothness mechanism in Table 3 yields the lowest jerk, and Table 4 highlights improved mission success with rapid convergence.

Table 8 Performance evaluation of the proposed framework under varying UAV sizes

UAV count	Mission success rate (%)	Avg path length (m)	Avg mission time (s)	Trajectory error (m)	Smoothness index	Collision rate (%)
10	98.5	41.7	31.6	0.83	0.89	3.6
25	98.2	42.6	33.9	0.87	0.88	4.0
50	97.9	43.8	36.4	0.92	0.87	4.4
75	97.6	44.9	38.8	0.96	0.85	4.8
100	97.2	46.0	41.2	1.00	0.84	5.2

Table 9 Computational complexity analysis with existing methods

Method	Flops (G)	Parameters (M)	Computation time (sec)	Energy consumption (J)	Memory usage (MB)
DDQN [9]	42.6	3.2	35.4	12.5	35
PPO + LSTM [10]	39.1	4.0	38.2	14.3	38
RL-CN [11]	41.3	3.8	33.1	13.7	41
K-MORP [12]	44.8	4.2	31.7	15.2	43
F2MGDRL-AEAO (proposed)	38.5	2.9	24.5	10.2	45

Table 10 Ablation study analysis on F2MGDRL components

Method	Mission success rate (%)	Average trajectory error (m)	Smoothness index	Real-time responsiveness (s)
Baseline MADRL	85.4	1.43	0.68	45
W/O FL	90.1	1.25	0.73	48.9
W/O Meta	92.5	1.18	0.76	47.2
W/O GNN	91.4	1.22	0.71	46.8
W/O AEAO	93.2	1.15	0.79	47.5
Proposed F2MGDRL	98.7	0.92	0.86	43.1

Even in high-complexity settings (Table 5), it outperforms centralized methods. Stability is verified in Table 6 through low variance, and Table 7 confirms efficient communication. The framework shows scalability, adaptive learning, and real-time capability with a 45 s processing time, proving resilient to environmental and communication uncertainties. However, initial model training is computationally demanding, and real-time navigation remains sensitive to extreme environmental uncertainties.

6 Conclusion

In this research, a hybrid deep learning-based real-time navigation framework was developed to enhance UAV performance in dynamic urban environments. The proposed system integrates a multi-objective cost function with FF2MGDRL and AEAO for smooth and reliable trajectory planning. Cellular network signals are leveraged to overcome GPS limitations, while 3DGCPM effectively mitigates intercell interference. The framework enables decentralized training across UAVs, ensuring data privacy, rapid adaptability, and robust coordination under varying environmental conditions. Performance evaluation confirms strong results, including a 98.7% mission success rate, 45 s processing time, 99.95% reliability, low trajectory error, and high smoothness with excellent real-time responsiveness. These outcomes demonstrate superior stability, reduced control chatter, and consistent navigation efficiency even in challenging scenarios. Future work will focus on real-world large-scale deployment, enabling heterogeneous multi-UAV cooperation, and incorporating energy-aware learning strategies. Additionally, the integration of emerging 6G communication technologies will be explored to enhance connectivity, reduce latency, and support intelligent air traffic management, further improving the safety and efficiency of autonomous UAV operations.

Acknowledgements None.

Author Contributions Tamilselvi P: conceptualization, methodology, validation. Jose Reena K: project administration, supervision, investigation. M. Vidhyasree: writing—original draft, writing—review and editing. Vishwa Priya V: supervision, investigation.

Funding This research did not receive any specific grant from funding agencies in the public, commercial, or not-for-profit sectors.

Data Availability Data sharing not applicable to this article as no datasets were generated or analyzed during the current study.

Declarations

Conflict of interest The authors declare that they have no potential conflict of interest.

Ethical Approval All applicable institutional and/or national guidelines for the care and use of animals were followed.

Informed Consent For this type of analysis, formal consent is not needed.

References

1. Bai K, Wu J, Wu H (2024) High-precision time synchronization algorithm for unmanned aerial vehicle ad hoc networks based on bidirectional Pseudo-range measurements. Ad Hoc Netw 152:103326
2. Díez-González J, Ferrero-Guillén R, Verde P, Martínez-Gutiérrez A, Álvarez R, Torres-Sospedra J (2024) Time-based UWB localization architectures analysis for uavs positioning in industry. Ad Hoc Netw 157:103419
3. Kundu J, Alam S, Dey A (2024) Fuzzy based trusted malicious unmanned aerial vehicle detection using in flying ad-hoc network. Alex Eng J 99:232–241
4. Ayad A, Bouzar Essaidi A, Haddad M (2025) Minimum-time trajectory planning for hexarotor UAV using random-profile approach. Int J Adv Manuf Technol 139:2719–2733
5. Suanpang P, Jamjuntr P (2024) Optimizing autonomous UAV navigation with D* algorithm for sustainable development. Sustainability 16:7867
6. Samma H, El-Ferik S (2024) Autonomous UAV visual navigation using an improved deep reinforcement learning. IEEE Access 12:79967–79977
7. Zhang J, Xian Y, Zhu X, Deng H (2025) A hybrid deep learning model for UAV path planning in Dynamic Environments. IEEE Access 13:67459–67475
8. Liu X, Zhong W, Wang X, Duan H, Fan Z, Jin H, Huang Y, Lin Z (2024) Deep reinforcement learning-based 3D trajectory planning for cellular connected UAV. Drones 8:199
9. Afifi G, Gadallah Y (2025) Autonomous real-time smoothness control for reliable DDQN-based UAV navigation using Cellular Networks. IEEE Access 13:22011–22028
10. Tonti F, Rabault J, Vinuesa R (2025) Navigation in a simplified urban flow through deep reinforcement learning. J Comput Phys 538:114194
11. Zhang L, Yi W, Lin H, Peng J, Gao P (2024) An efficient reinforcement learning-based cooperative navigation algorithm for multiple uavs in complex environments. IEEE Trans Ind Inform 20:12396–12406
12. Ren Z, Hussain K, Faheem M (2024) K-means online-learning routing protocol (K-MORP) for unmanned aerial vehicles (UAV) adhoc networks. Ad Hoc Netw 154:103354
13. Meng Q, Song Y, Li S, Zhuang Y (2023) Resilient tightly coupled INS/UWB integration method for indoor UAV navigation under challenging scenarios. Def Technol 22:185–196
14. Tricomi G, Scaffidi C, Puliafito A, Distefano S (2024) CV pop-corn: the (SMART) city-vehicle participatory-opportunistic cooperative route navigation system. Ad Hoc Netw 164:103604
15. Pasandideh F, Najafzadeh A, da Costa JPJ, Santos GA, de Lima DV, de Freitas EP (2025) Providing an energy efficient UAV BS positioning mechanism to improve wireless connectivity. Ad Hoc Netw 170:103767
16. Tutsoy O, Asadi D, Ahmadi K, Nabavi-Chashmi SY, Iqbal J (2024) Minimum distance and minimum time optimal path planning with bioinspired machine learning algorithms for faulty unmanned air vehicles. IEEE Trans Intell Transp Syst 25:9069–9077
17. Wang M, Chen X, Wang S, Shi W (2025) Three-dimensional geometry-based channel modeling and simulations for reconfigurable intelligent surface-assisted uav-to-ground MIMO communications. IET Commun. https://doi.org/10.1049/cmu2.12724
18. Ficco M, Guerriero A, Milite E, Palmieri F, Pietrantuono R, Russo S (2024) Federated learning for IOT devices: enhancing tinyml with on-board training. Inf Fusion 104:102189
19. Wang C, Shen X, Zhang Z, Tao C, Xu Y (2025) Cross-scene multi-object tracking for drones: leveraging meta-learning and onboard parameters with the new MIDDTD. Drones 9:341
20. Ma Z, Xiong J, Gong H, Wang X (2024) Adaptive depth graph neural network-based dynamic task allocation for UAV-ugvs under complex environments. IEEE Trans Intell Veh 10(5):3573–3586
21. Xue Y, Chen W (2023) Multi-agent deep reinforcement learning for uavs navigation in unknown complex environment. IEEE Trans Intell Veh 9:2290–2303
22. Rodan A, Al-Tamimi A-K, Al-Alnemer L, Mirjalili S, Tiňo P (2025) Enzyme action optimizer: a novel bio-inspired optimization algorithm. J Supercomput. https://doi.org/10.1007/s11227-025-07052-w
23. Abdel-Basset M, Mohamed R, Abouhawwash M (2024) Crested porcupine optimizer: a new nature-inspired metaheuristic. Knowl-Based Syst 284:111257
24. Wang X, Snášel V, Mirjalili S, Pan J-S, Kong L, Shehadeh HA (2024) Artificial protozoa optimizer (APO): a novel bio-inspired metaheuristic algorithm for engineering optimization. Knowl-Based Syst 295:111737
25. Bouaouda A, Hashim FA, Sayouti Y, Hussien AG (2024) Pied kingfisher optimizer: a new bio-inspired algorithm for solving numerical optimization and industrial engineering problems. Neural Comput Appl. https://doi.org/10.1007/s00521-024-09879-5